Conformation of T4 Lysozyme in Solution. Hinge-Bending Motion and the Substrate-Induced Conformational Transition Studied by Site-Directed Spin Labeling†

Hassane S. Mchaourab, Kyoung Joon Oh, Celia J. Fang, and Wayne L. Hubbell*

Jules Stein Eye Institute and Department of Chemistry and Biochemistry, University of California, Los Angeles, California 90095-7008

Received August 21, 1996; Revised Manuscript Received October 23, 1996⊗

ABSTRACT: T4 lysozyme and mutants thereof crystallize in different conformations that are related to each other by a bend about a hinge in the molecule. This observation suggests that the wild type protein may undergo a hinge-bending motion in solution to allow substrate access to an otherwise closed active site cleft [Faber, H. R., & Matthews, B. W. (1990) *Nature 348*, 263−266]. To test this hypothesis, either single or pairs of nitroxide side chains were introduced into the protein to monitor tertiary contact interactions and inter-residue distances, respectively, in solution. A set of constraints for these structural parameters was derived from a reference state, a covalent enzyme−substrate adduct where the enzyme is locked in the closed state. In the absence of substrate, differences in both inter-residue distances and tertiary contact interactions relative to this reference state are consistent with a hinge-bending motion that opens the active site cleft. Quantitative analysis of spin−spin interactions between nitroxide pairs reveals an 8 Å relative domain movement upon substrate binding. In addition, it is demonstrated that the I3P mutation, which produces a large hinge-bending angle in the crystal, has no effect on the solution conformation. Thus, the hinge motion is not the result of the mutation but is an integral part of T4 lysozyme catalysis in solution, as suggested recently [Zhang, X. J., Wozniak, J. A., & Matthews, B. W. (1995) *J. Mol. Biol. 250*, 527−552]. The strategy employed here, based on site-directed spin labeling, should be generally applicable to the study of protein conformation and conformational changes in solution.

Proteins are intrinsically flexible structures that can exist in multiple conformations in solution. If the conformers are well separated in energy, transitions between them can be induced by an interaction with the surroundings, such as substrate binding, modulation of an electric field intensity, etc. If conformers have similar energies, multiple states may be thermally populated in solution at equilibrium. In either case, protein function may be mediated by conformational transitions, and elucidation of structure−function relationships requires experimental strategies capable of resolving conformational states in solution.

For states with similar energies, lattice energies may be sufficiently large to effectively select a particular state in a crystal, obscuring the existence of others (Bennett & Huber, 1984). Thus, X-ray crystallographic methods are not generally suited to identifying conformeric equilibria, although the existence of such equilibria has been inferred from studies of thermal factors (Weaver & Matthews, 1987) and multiple crystal forms (Petsko & Ringe, 1984; Faber & Matthews, 1990; Bennett & Steitz, 1978). Solution structures of proteins determined from high-resolution NMR reveal differences from the crystal structures (Wagner et al., 1992), but at present, NMR is limited to low-molecular weight proteins and is not generally applicable to membrane proteins.

Site-directed spin labeling (SDSL)[1] is emerging as a powerful technique for exploring the structure and dynamics of both soluble and membrane proteins of any molecular weight [see Hubbell and Altenbach (1994) and Hubbell et al. (1996) for recent reviews]. Conformational transitions that result in repacking along tertiary contact interfaces can be detected as a change in the dynamics of suitably placed spin-labels (Mchaourab et al., 1996). For example, Steinhoff et al. (1994) and Farahbakhsh et al. (1993) have shown that SDSL can provide a time-resolved view of triggered protein conformational transitions in bacteriorhodopsin and rhodopsin, respectively. In addition, rigid body motion of entire domains or secondary structural units can be detected as a change in the distance between pairs of nitroxides in frozen solution (Farrens et al., 1996). Spin−spin interaction between pairs of nitroxides can also be used to monitor spatial proximity at room temperature (Fiori et al., 1993). In this paper, we extend these SDSL tools to study intrinsic protein flexibility and to examine differences between the crystal and solution structures of T4L.

T4L is a 164-residue globular protein consisting of two domains connected by a long α-helix. The enzyme cleaves the glycosidic bond between *N*-acetylmuramic acid and *N*-acetylglucosamine of the bacterial cell wall saccharide. In the X-ray structure of the WT protein, the active site, located in a cleft between the N-terminal and the C-terminal domains, appears to be occluded and inaccessible to the

† Research reported here was supported by NIH Grant EY05216 (W.L.H.), Research to Prevent Blindness (W.L.H.), and the Jules Stein Professorship Endowment (W.L.H.).

* To whom correspondence should be addressed.

⊗ Abstract published in *Advance ACS Abstracts,* December 15, 1996.

[1] Abbreviations: EPR, electron paramagnetic resonance; MOPS, morpholinopropanesulfonic acid; SDSL, site-directed spin labeling; T4L, T4 lysozyme; WT, wild type.

S0006-2960(96)02114-9 CCC: $14.00

substrate. However, analysis of thermal factors led to the hypothesis that conformational fluctuations might occur in solution to open the active site cleft and allow substrate binding (Weaver & Matthews, 1987). Moreover, the X-ray structures of mutants I3P and M6I reveal a relative rotation of the N- and C-terminal domains about a hinge site by up to 32° with respect to the wild type, opening the active site cleft by up to 8 Å (Faber & Matthews, 1990; Dixon et al., 1992).

Whether these extreme conformations reflect states populated in solution is not known. Arnold et al. (1994) carried out a molecular dynamics simulation of the hinge-bending motion of T4L. Although relative motion between the two domains was evident, the magnitude was smaller than that suggested by the various crystal structures of the mutants. Initially, Matthews and co-workers suggested that the large hinge-bending angle observed in the structure of I3P and M6I may be a consequence of repacking due to the mutations (Dixon et al., 1992). On the other hand, both mutations are close to sites of extensive interprotein contacts in the crystal, and lattice forces may be responsible for the different structures. Recently, Zhang et al. (1995) reported that the conformation of T4L with a mutation distant from the hinge-bending locus displays an angle of rotation as large as the one seen in the structure of mutants M6I and I3P and suggested that hinge-bending may be an intrinsic property of T4L.

To examine the conformation of T4L in solution, spin-labeled side chains have been introduced into regions of the molecule that show large conformational differences between the WT (crystallographic "closed" state) and its hinge-bending mutants I3P or M6I (crystallographic "open" states). The dynamics of single nitroxide side chains and patterns of spin−spin interactions between pairs of nitroxides in T4L in solution reveal a conformeric equilibrium involving a significant population of an open conformation. To provide a quantitative estimate of the magnitude of domain movements in solution, we analyzed the mechanism of spin−spin interaction at room temperature using pairs of nitroxides introduced at known distances in T4L. The distance dependence of the observed spin−spin interactions reveals that the dominant mechanism is the modulation of the anisotropic electron dipole−dipole interaction by rotational motion of the interspin vector. Using this experimental proximity scale, the transition from the closed to the open state is shown to result in an opening of the active site cleft of 8 Å. In addition, we have found that introduction of the I3P mutation does not significantly change the relative orientation of the two domains in solution. The data presented in this paper support the hypothesis of Zhang et al. (1995) that the conformational flexibility observed in the crystal structures of various T4L mutants is not a consequence of mutation and that hinge-bending is an intrinsic property of T4L in solution.

MATERIALS AND METHODS

Materials. Spin-label (**I**) [(1-oxy-2,2,5,5-tetramethylpyrrolinyl-3-methyl)methanethiosulfonate] (Figure 1) was a generous gift from Prof. K. Hideg (University of Pecs, Hungary). Restriction enzymes were from Promega (Madison, WI). Resource S and Superdex 75 columns were from Pharmacia (Piscataway, NJ).

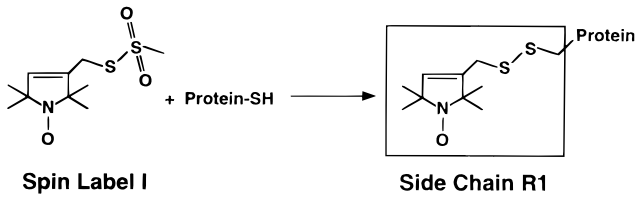

FIGURE 1: Reaction of the methanethiosulfonate spin-label (I) with cysteine to generate side chain R1.

Construction and Purification of Spin-Labeled Lysozyme. Mutant lysozymes were constructed as previously described (Mchaourab et al., 1996). Double cysteine mutants were constructed by subcloning using the appropriate restriction endonucleases. The sequences of all mutants were verified by DNA sequencing. The expression and purification of mutant lysozymes and their quantitative modification with spin-label (**I**) to generate the nitroxide side chain R1 (Figure 1) were carried out as previously described (Mchaourab et al., 1996).

Mutant lysozymes containing a covalently linked substrate were produced by introducing the mutation T26E, and the enzyme−substrate complex was purified by cation exchange chromatography on a Resource S column (Kuroki et al., 1993), followed by gel filtration on a Superdex 75 column. The purified protein contained less than 10% substrate-free protein as determined by SDS−PAGE. In some experiments, the substrate was removed from the T26E mutant by acid hydrolysis at 37 °C (Kuroki et al., 1993).

EPR Measurements and Analysis of Spectra. EPR spectroscopy was performed on a Varian E-109 spectrometer as previously described (Mchaourab et al., 1996). For analysis of spin−spin interactions in double mutants, EPR spectra were recorded at room temperature in a buffer containing 10 mM MOPS, 100 mM NaCl, and 0.1 mM EDTA at pH 7.5. For analysis of nitroxide side chain dynamics in single mutants, spectra were recorded in the same buffer containing 30% w/v sucrose. This has the effect of increasing the protein correlation time by a factor of about 3, a condition under which the spectral line shapes reflect motion of the nitroxide relative to the protein (Mchaourab et al., 1996).

The experiments presented below involve detection of spin−spin interaction in mutants of T4L containing two nitroxide side chains. As discussed below, the primary mechanisms of spin−spin interaction in the cases considered here are weak through-space exchange (Fiori et al., 1993; Fiori & Millhauser, 1995), static-dipolar (Farahbakhsh et al., 1995; Rabenstein & Shin, 1995), and modulation of the dipolar interaction by molecular tumbling (Abragam, 1961), each of which leads to distance-dependent broadening of the EPR spectrum in an isotropic distribution of nitroxides. Such spectral broadening due to spin−spin interaction is readily detected by an amplitude decrease (and line width increase) in the EPR spectrum of the doubly labeled mutant with respect to the sum of the EPR spectra of the single mutants. For this comparison, the EPR spectra were normalized to represent the same number of spins.

Estimation of Interspin Distances from Modeling. Despite the relatively long linker connecting the nitroxide ring to the backbone in side chain R1 (Figure 1), the nitroxide ring has a highly restricted range of motion at helix surface sites. This results from immobilization of the $C_\alpha-C_\beta-S-S$ segment on the EPR time scale, apparently due to interaction of the disulfide group with main chain atoms in the helix.

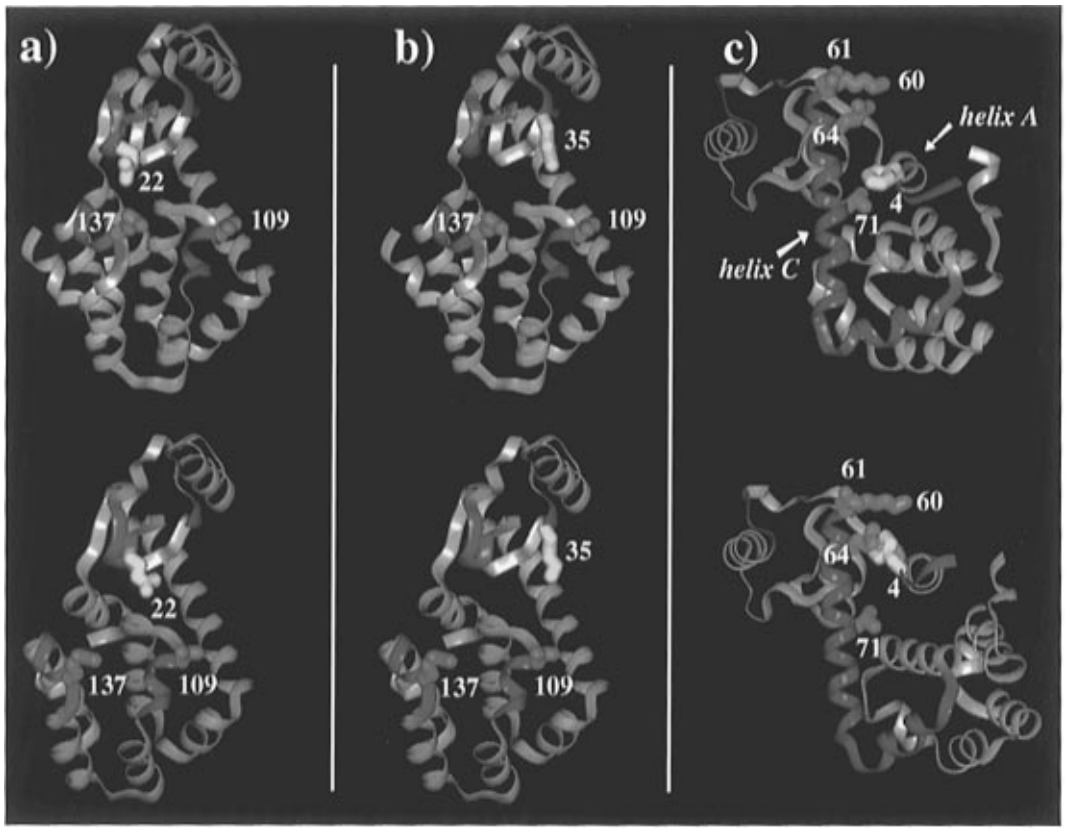

FIGURE 2: Crystal structures of T4L in the closed (wild type) and open (M6I) conformations showing selected side chains. In each panel, the upper structure is the closed state and the lower structure the open state. Panel a shows a view of the active site cleft, indicating the position of reference residue 22 relative to residues 109, and 137 in the closed and open states. Panel b is the same view as a, indicating the position of reference residue 35 relative to residues 109 and 137 in the closed and open states. Panel c shows a view of the packing interface of helices A and C and indicates the position of residue 4 relative to residues 60, 61, 64, and 71 in the closed and open states.

On the basis of this information, a conformation of the R1 side chain with the disulfide lying fixed along the backbone was suggested (Mchaourab et al., 1996). To estimate distances between the nitroxide groups at helix sites, R1 side chains in this conformation were introduced into the T4L structure and energy minimized with respect to the conformation of the side chain and steric interactions (Insight II, CVFF force field). For the R1 side chain loop sites, the conformation of the side chain was determined by energy minimization with respect to side chain conformation and steric interactions with main chain and side chain atoms. Probable ranges for interspin distances were estimated from the range of structures with roughly equal conformational energies.

RESULTS

Inter-Residue Distances in the Crystallographic Open and Closed Conformations of T4L and the Rationale for the Experimental Approach. One goal of these experiments is to test the hypothesis that the conformation of T4L in solution more closely resembles the crystal structure of the M6I mutant with an open active site cleft than it does the WT structure with a closed active site cleft. A direct approach to this end is the determination of inter-residue distances for selected pairs of sites that clearly distinguish the two conformations. Here we employ pairs of nitroxide side chains introduced at selected sites to compare inter-residue distances *via* the EPR spectral broadening that results from distance-dependent spin−spin interactions.

Each of the three panels of Figure 2 shows a pair of structures, the upper of which is the crystallographic closed conformation (WT T4L) and the lower of which is the open conformation (M6I, molecule C). In each pair, the open and closed structures were aligned in the N-terminal domain (residues 15−60). The difference between the closed and open states involves a rigid body rotation of one domain relative to the other that is most clearly seen in Figure 2c. Although the structural integrity of each domain is maintained, there are alterations in the spatial proximity of entire polypeptide segments across the active site cleft and changes in the relative alignment of helices A and C. The deviation in the backbone conformation between the two structures can be quantitatively expressed using a displacement plot (Dixon et al., 1992). On the basis of this plot, sites were selected for introduction of pairs of nitroxide side chains. We refer to the double mutants with the notation RXR1/R′X′R1, where R and R′ are the original residues at positions X and X′, respectively, and R1 is the spin-labeled side chain.

The locations of the individual sites selected for labeling are shown in Figure 2. In each case, one member of the pair was selected to lie in the N-terminal domain (residues 4, 22, and 35), with the other in a region that undergoes relative displacement upon hinge-bending (residues 60, 61, 64, 71, 109, and 137). Where possible, the sites were restricted to solvent-exposed surface locations where the R1 side chain has a high mobility and causes little or no structural perturbation (Mchaourab et al., 1996). The pairwise sites were selected to provide a distinctive *pattern* of distance changes unique to the closed−open transformation. For example, in going from the closed to the open state, the distance 22 to 109 decreases, but that from 22 to 137 increases (Figure 2a). The distance from 35 to 137 increases,

but that from 35 to 109 remains approximately constant (Figure 2b). The distance from 4 to the triad 60, 61, and 64 decreases, while that from 4 to 71 increases (Figure 2c).

Selection of multiple pairs of sites predicted to change in a distinctive pattern has the advantage of the fact that a specific model can be tested by observing experimentally only the *sign* of the relative displacement between pairs. This in turn is readily deduced from the qualitative change in EPR spectral broadening due to spin−spin interactions; i.e., a decrease in broadening implies an increase in distance and *vice versa*. In the results to follow, the experimental *pattern* of interspin distance changes between T4L in solution with and without bound substrate is compared to those shown in Figure 2.

This "pattern approach" is emphasized here because we anticipate applications where quantitative analysis of EPR spectra of interacting spin pairs in terms of distance is not possible due to the lack of appropriate theory. Nevertheless, it is clearly useful to analyze interactions in terms of absolute distance where possible, and we include a quantitative analysis of interspin distances that extend and strengthen the conclusions deduced from the pattern approach.

Distance measurement provides an obvious means for mapping structural changes. However, the mobilities of single R1 side chains in a protein are closely correlated with the extent of tertiary interactions at a particular site and can thus be used as a sensitive measure of conformational differences between states of a protein (Mchaourab et al., 1996). This strategy is also employed here to examine structural changes induced by the presence of bound substrate in T4L.

Closed Conformation in Solution. The mutant T26E forms a covalently linked enzyme−substrate complex with a slightly negative hinge-bending angle in the crystal structure (Kuroki et al., 1992). Within the resolution of the studies presented here, it has the closed conformation of the WT crystal structure; i.e., the spatial proximities between the sites selected for labeling are expected to be similar. In solution, the T4L−substrate complex is locked in the closed conformation and is used as a reference state for interpretation of EPR data.

The heavy trace in Figure 3 shows EPR spectra for the indicated double mutants with bound substrate, while the light trace shows the sum of the spectra for the corresponding single mutants. In all but D22R1/T109R1, a significant broadening and concomitant loss of intensity are observed in the EPR spectra of the double mutants with respect to the sums of the spectra of the corresponding single mutants, demonstrating spin−spin interactions between the nitroxides. For convenience of presentation, the spectra of the double mutants were scaled to show the details of the line shape. The results are consistent with the known structure of the closed conformation. For example, the interspin distance between the nitroxides in D22R1/T109R1 is estimated from molecular modeling to be about 21 Å, near the limit of detection for magnetic dipolar interactions between the nitroxides (see below), consistent with the weak spin−spin interaction. For D22R1/R137R1 and F4R1/V71R1, molecular modeling suggests that the nitroxide groups are near van der Waal's contact, consistent with the extreme broadening of the corresponding spectra. The distances between the nitrogen atoms of the nitroxides in K35R1/T109R1, K35R1/R137R1, and F4R1/K60R1 are estimated from molecular modeling to be ≈13, 14, and 17 Å, respectively, consistent

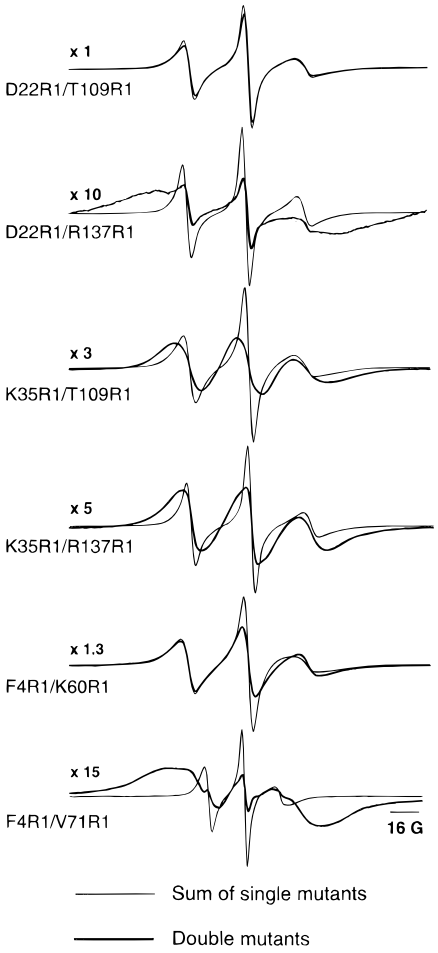

FIGURE 3: Room-temperature EPR spectra of spin-labeled mutants of T4L with bound substrate (T26E mutation). The light trace is the sum of the single-mutant spectra. The heavy trace is the double-mutant spectrum normalized to the same number of spins as the corresponding sum of singles and then scaled for convenience of presentation. The scaling factor is shown to the left of the spectra. All spectra were recorded with a 100 G scan width, except F4R1/V71R1, which had a magnetic field scan width of 160 G.

with an intermediate degree of spectral broadening, relative to the sum of the spectra of the single mutants, as observed.

T4L Conformation in the Absence of Substrate. Figure 4a compares the spectra of the double mutants with (heavy trace) and without (light trace) bound substrate, and Figure 4b makes the same comparison for the sum of the spectra of the corresponding single mutants. The spectral differences in the single mutants reveal changes in nitroxide mobility associated with substrate binding. In all cases except K35R1/T109R1, the differences between spectra of a given double mutant due to substrate binding clearly exceed those in the sum of the spectra of the single mutants. Furthermore, the changes in the double mutant spectra involve new features (indicated by the arrows in Figure 4) that cannot arise from changes in mobility. Thus, the spectral differences in the double mutants due to the presence of substrate are not due to differences in side chain mobilities but are rather due to spin−spin interaction and hence indicate changes in interspin distances. Under any circumstance, significant changes in side chain mobility due to substrate binding are seen only in the spectral sums D22R1 + T109R1 and K35R1 + T109R1, and they are rather small. Note that for D22R1 + T109R1 mobility changes cause a decrease in spectral amplitude with substrate binding but an increase in amplitude for the double mutant D22R1/T109R1. Therefore, mobility

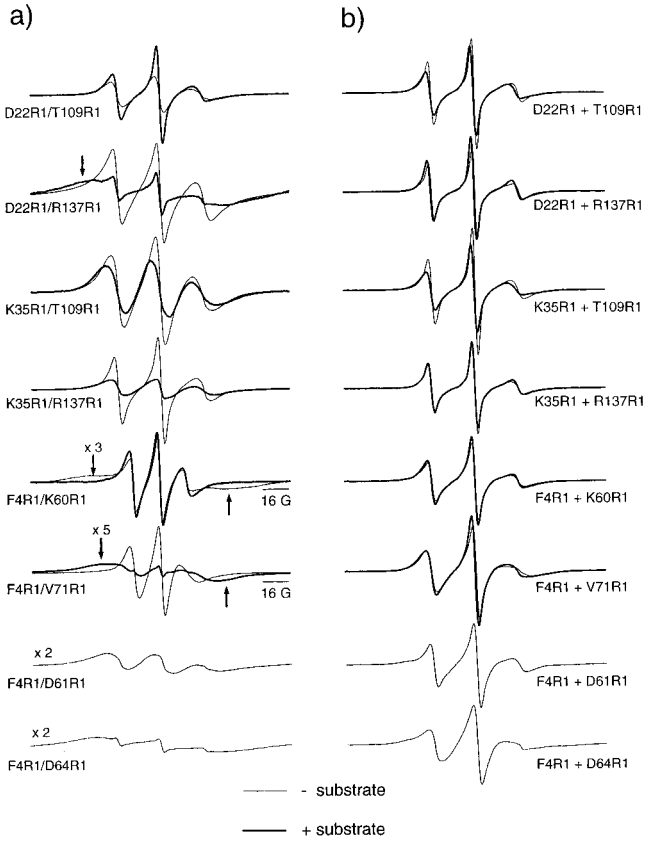

FIGURE 4: Room-temperature EPR spectra of spin-labeled mutants of T4L with and without bound substrate: (a) EPR spectra of the indicated double mutants of T4L with (heavy trace) and without (light trace) bound substrate and (b) the sum of the EPR spectra of the single mutants corresponding to a with (heavy trace) and without (light trace) bound substrate. For each pair of spectra, except F4R1/D61R1 and F4R1/D64R1, the spectra are normalized to represent the same number of spins, except where noted by a scaling factor. The spectra of F4R1/D61R1 and F4R1/D64R1 (a) and their corresponding sum of singles (b) were normalized to respresent the same number of spins and then scaled to show details of the line shape. The protein with bound substrate is the T26E mutant. All spectra were recorded with 100 G scan widths, except F4R1/V71R1 (a) and F4R1/D60R1 (a), which have a scan width of 160 G.

effects act to reduce the magnitude of distance effects. In the double mutant K35R1/T109R1, the effect of substrate binding is relatively small, and the difference has some contribution from the mobility effects noted in the spectral sum of K35R1 + T109R1.

Inter-residue distance changes, having been established as the origin of the spectral line shape changes, can now be interpreted in terms of structural differences between the substrate-bound and substrate-free forms of T4L. The increase and decrease in spectral widths of D22R1/T109R1 and D22R1/R137R1, respectively, relative to the substrate-bound closed state, indicate a movement of T109R1 toward and R137R1 away from D22R1. In the same context, R137R1 moves away from K35R1, while the distance between K35R1 and T109R1 changes little but could increase slightly. An examination of panels a and b of Figure 2 shows that this pattern of distance changes upon substrate removal is consistent with a transition from the closed to a more open state resembling that of the M6I mutant. Thus, these data are in accord with a global rigid body rotation of one domain relative to the other upon substrate binding, rather than limited local rearrangements in the polypeptide.

In addition to the above changes near the active site cleft, removal of the substrate dramatically decreases the interaction between nitroxides in R4R1/V71R while increasing the interaction between those in F4R1/K60R1, as shown by the appearance of a broad spectral component indicated by arrows in Figure 4a. One of the most striking changes in the closed−open transition is the repacking of the interface between helices A and C. As a consequence, residue F4 moves away from V71 and toward K60, precisely the change observed in the EPR spectra. Additionally, the mutants F4R1/D61R1 and F4R1/D64R1 show strong spin−spin interaction in the absence of substrate, confirming the proximity of residue 4R1 to residues D61 and D64 near the N terminus of helix C (Figure 2c). Collectively, these results strongly support the existence of an open conformation of the enzyme in solution in the absence of substrate.

The above experiments compare the EPR spectra of double mutants containing the T26E substitution, with bound substrate, to the spectra of a double mutant constructed in the WT T4L background. Similar changes in the spectra were obtained when the substrate was removed by acid hydrolysis using the method of Kiroki et al. (1993) (data not shown). That is to say, the T26E mutation itself has little effect on the conformation of T4L in solution.

While the spectra in the presence of substrate can be accounted for by the interaction of two spins at a single distance, the spectra in the absence of substrate are more complex and suggest a conformational heterogeneity that may arise from an equilibrium mixture of states. This is most clearly revealed in the spectrum of F4R1/K60R1, where very broad (arrows) and narrow components suggest at least two populations, one with the spins in close proximity and the other with the spins at a much larger distance. The broad component, corresponding to an open state, is dominant in terms of spin population. In the spectra of D22R1/R137R1 and F4R1/D61R1, the existence of multiple components is suggested by the "wings" of the spectra that give resonance intensity with a breadth of nearly 100 G, although the central features of the spectrum are relatively narrow. This point is considered further in the Discussion.

Effect of the I3P Mutation on the Solution Structure. Domain movement in T4L was initially detected in the comparison of the wild type crystal structure with those of the mutants I3P and M6I. The location of these mutations near the putative hinge-bending axes suggested that they may be at the origin of the rather large hinge-bending angle observed. To determine whether the I3P substitution has any effects on the conformation(s) in solution, the I3P mutation was introduced into the double mutants D22R1/N141R1 and D22R1/R137R1, both of which have interspin distances that are a function of the hinge-bending angle. In fact, D22R1/R137R1 shows one of the largest changes observed upon hinge-bending (Figure 4). As shown by the EPR spectra in Figure 5, only small changes are caused by the introduction of the I3P mutation. This is particularly significant because the strong distance dependence of any of the spin−spin interaction mechanisms would result in large spectral changes for even small displacements. The changes observed are sufficiently small to permit the conclusion that the I3P mutation causes little, if any, shift in conformeric equilibria in solution.

Analysis of Side Chain Dynamics. In addition to changes in inter-residue distances, hinge-bending motions are also

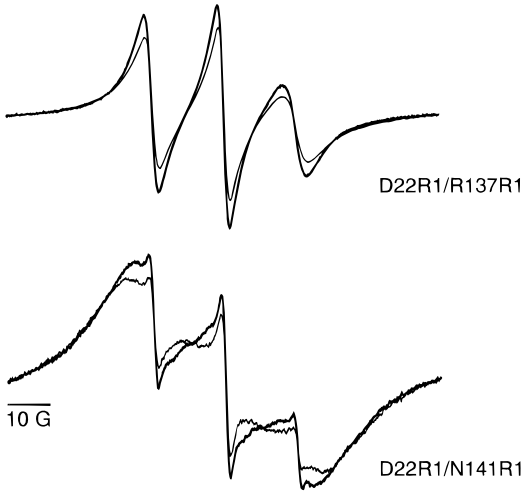

FIGURE 5: Effect of the I3P mutation on the conformation of T4L near the active site cleft. Light traces correspond to the spectrum of the indicated double mutants. Heavy traces correspond to the I3P variant of each mutant. All spectra were recorded with a 100 G scan width.

expected to result in changes in tertiary interactions of specific side chains. As shown previously, changes in tertiary contact interactions are reflected in the dynamics of single nitroxide side chains and hence in the EPR spectral line shape (Mchaourab et al., 1996). Thus, analysis of spectral line shape changes provides a complementary strategy for analyzing the solution conformations in T4L relative to those in the T4L−substrate complex.

The EPR spectral line shapes reflect the motion of the nitroxide side chain relative to the protein as well as the tumbling of the protein molecule as a whole. To observe the motion of the side chain relative to the protein, the tumbling of the protein must be largely eliminated in terms of its effect on the EPR spectral line shape. This can be achieved without altering the motion of the individual side chains by increasing the viscosity of the medium (Timofeev & Teltsin, 1983). For T4L, a viscosity of 0.03 P (30% sucrose) at room temperature is sufficient for this purpose (Mchaourab et al., 1996).

Figure 6 shows the EPR spectra in 30% sucrose for a set of mutants containing single nitroxide side chains at the indicated positions, both in the T4L−substrate complex and in T4L alone. Sites 4 and 71 were selected to represent regions of the molecule that undergo significant changes in tertiary interaction upon transition from the closed to open state. Thus, F4 moves from a solvent-exposed site in the closed state to a site buried at the contact face of the A and C helices in the open state. Concomitantly, V71 moves in the opposite sense, from a buried site at the contact face of these helices to a solvent-exposed site. Comparison of the EPR spectra of F4R1 and V71R1 in the T4L−substrate complex and T4L in solution demonstrates that these changes in fact take place upon removal of substrate; the spectrum of F4R1 in the T4L−substrate complex is characteristic of a rapid anisotropic motion of a single solvent-exposed spin population, while that in T4L has multiple components, one of which is highly immobilized, resulting from tertiary contact interaction (Figure 6, arrow). On the other hand, the spectrum of V71R1 in the T4L−substrate complex indicates a highly immobilized state, consistent with the expected buried location. In T4L, the spectrum is that of a mobile, solvent-exposed site, reflecting the open state.

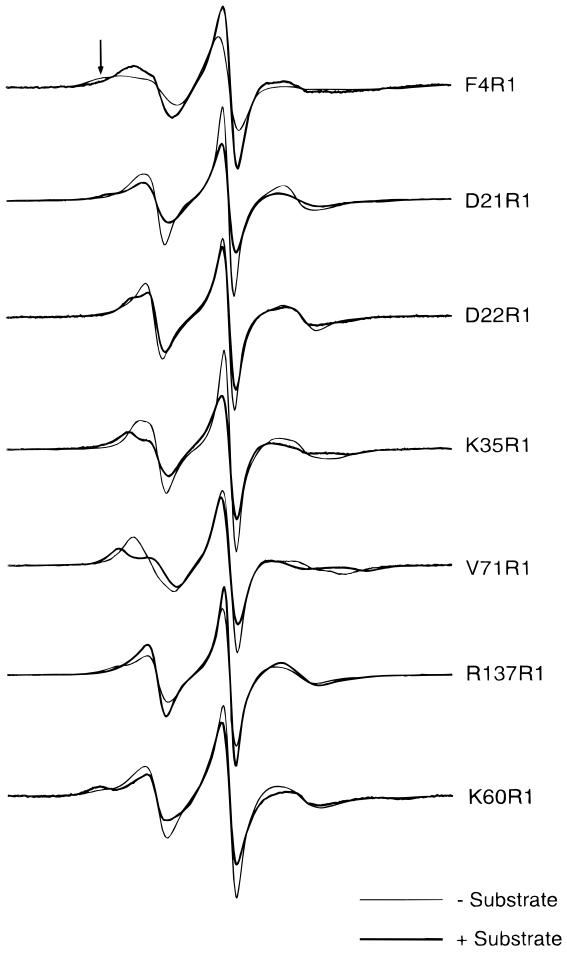

FIGURE 6: EPR spectra of spin-labeled single cysteine mutants with (heavy trace) and without (light trace) bound substrate. The protein with bound substrate is the T26E mutant. All spectra were recorded in the presence of 30% sucrose with 100 G field scans.

Sites 21, 22, and 35 are located in interhelical loop structures. Each of these sites has EPR spectra that reflect significantly less mobility in the T4L−substrate complex than in T4L. This is likely to be the result of damped backbone fluctuations, because such fluctuations appear to be the dominant contribution to mobility at these sites (Mchaourab et al., 1996).

Residue 137 is at the N terminus of a helix. The nitroxide side chain R1 has been found to have characteristic two-component spectra at such sites, apparently due to hydrogen-bonding interactions with backbone amide residues (Mchaourab et al., 1996). While the two-component spectrum is observed in T4L, only a single component is observed in the T4L−substrate complex. This may result from competition for backbone H bond formation between the R1 side chain and the nearby substrate.

Residue 60 is located near the N terminus of helix C. In the T4L−substrate complex, a typical two-component N-terminal spectrum is observed for K60R1. In T4L, the spectrum reflects an increase in the population of the more mobile state. Faber and Matthews (1990) observed changes in backbone conformation associated with hinge bending around residues 13, 59, and 80, and this effect may be the origin of the observed spectral difference.

Single R1 side chains at locations not expected to undergo changes in tertiary contact interactions upon substrate removal (44 and 72) show no corresponding spectral changes (data not shown).

FIGURE 7: T4L structure showing the locations of spin-labeled mutants along the interdomain helix.

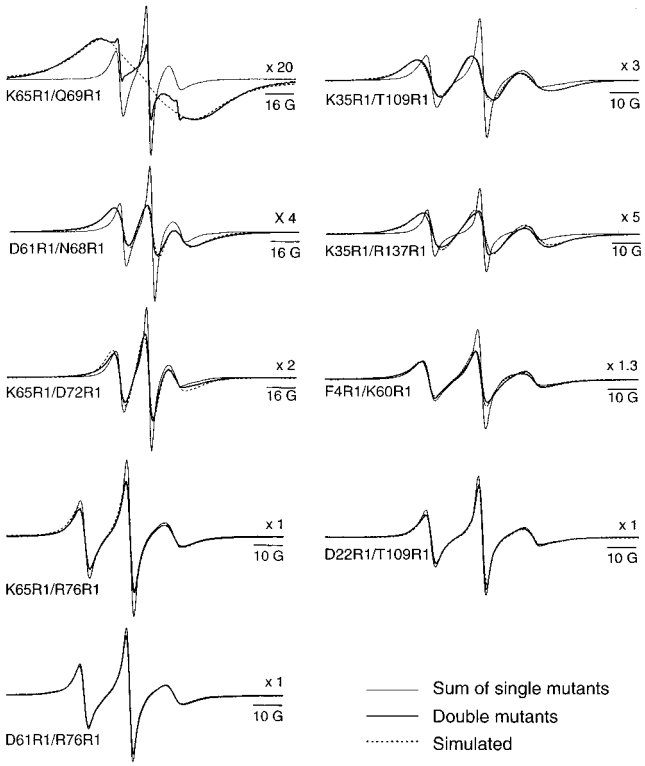

FIGURE 8: EPR spectra of the indicated double mutants (heavy trace), the sum of the corresponding single mutants (light trace), and the convolution of the sum of the singles with a Lorentzian broadening function that gives the best fit (dashed trace).

Estimation of the Distance between Nitroxide Side Chains. As shown above, qualitative analysis of the EPR spectral line broadening in the double mutants is sufficient to test specific models for domain movements in T4L. Nevertheless, quantitative information on interspin distances provides more information concerning the amplitude of the movements, and the spin pairs in the T4L molecule provide an opportunity to examine the quantitative aspects of the spectral line broadening. For this purpose, F4R1/K60R1, D22R1/T109R1, K35R1/T109R1, and K35R1/R137R1 in the closed state (substrate-bound) were selected, because the true interspin distances can be estimated from the crystal structure. In addition, a set of five double mutants was prepared with each member at a position along the exposed surface of the long interdomain α-helix extending from 61 to 80 (Figure 7). The inter-residue distances along this helix are not effected by hinge bending.

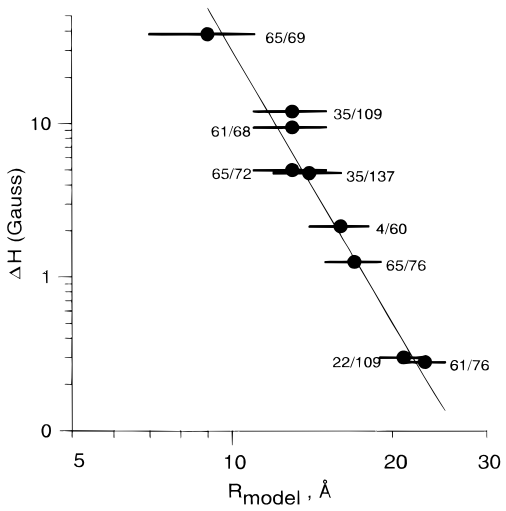

FIGURE 9: Plot of spectral broadening (ΔH) in the double mutant *versus* interspin distance (R_{model}). The spectral broadening was determined as described in the text, and R_{model} was estimated as described in Materials and Methods. The horizontal bars indicate the probable range of distances determined from modeling. The solid line is a least-squares best fit to the data given by $\Delta H = 2.3937 \times 10^6 R^{-5.9}$.

In each of these cases, the spectrum of the double mutant can be fit reasonably well by the convolution of a Lorentzian broadening function with the sum of the spectra of the corresponding single mutants, as shown by the dashed lines in Figure 8. Thus, the broadening due to spin−spin interaction is apparently homogeneous and uniform across the spectrum, and the line width at half-height (ΔH) of the Lorentzian giving the best fit provides a quantitative measure of the broadening and hence spin−spin interaction. A similar approach was used by Smirnov et al. (1996) to quantitate spectral broadening due to Heisenberg exchange.

Figure 9 shows a plot of ΔH determined in this fashion *versus* the interspin distance determined from molecular modeling. The width of the horizontal bars reflects the estimated range in the distances determined from modeling (see Materials and Methods). The solid line is a least-squares fit to the data and shows that ΔH is proportional to $1/r^6$ within experimental error. This plot can be used to estimate other distances in T4L from experimental values of ΔH. We illustrate this with one instructive example, the interspin distance in the double mutant K35R1/R137R1 in the open state, in the absence of substrate. In this case, $\Delta H \approx 0.4$ G, corresponding to an interspin distance of ≈21 Å. In the closed state, molecular modeling indicates that this same pair is separated by about 13 Å . Thus, the interdomain movement across the active site cleft in the closed−open transition is about 8 Å, the same value obtained from comparison of the crystallographic closed and open forms (Faber & Matthews, 1988).

It is of interest to consider possible mechanisms of spin−spin interaction that lead to the simple relationship in Figure 9. Nitroxide spins can interact with each other by exchange and/or dipolar interactions. Through-bond exchange is negligible for the mutants considered here because of the large number of bonds between nitroxide residues. Through-space exchange interaction has been modeled as an exponentially decreasing function with a space constant of less

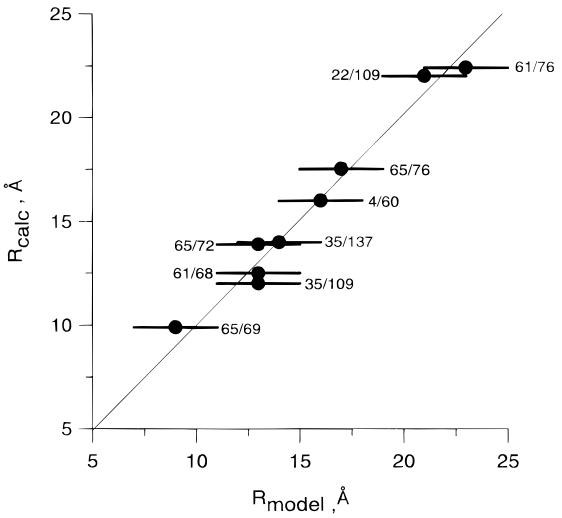

FIGURE 10: Comparison of interspin distance calculated by the rotational dipole mechanism (R_{calc}) to that determined by modeling (R_{model}). The slope of the line is 1.

than 1 Å and is expected to be completely negligible at separations of 14 Å and beyond (Fiori & Millhauser, 1993).

Dipole−dipole interactions between spin pairs can be either static or dynamic. For rotational correlation times of the protein of less than about $(3\pi g^2\beta^2/r^3h)^{-1}$, where g, β, h, and r are the electronic g factor, the Bohr magneton, the Planck constant, and the interspin distance, respectively, the static contribution is averaged. For spin pairs fixed in T4L, the correlation time for the interspin vector is that for protein rotation, ≈6 ns in water at room temperature. For this correlation time, static dipolar effects are averaged for interspin distances of ≥15 Å. In this regime of motional averaging, relaxation effects due to rotational modulation of the anisotropic dipole−dipole interaction come into play and may lead to homogeneous spectral line broadening, ΔH_{dd}, characterized by a transverse relaxation time, T_{2dd}, given by the following (Abragam, 1961)

$$\Delta H_{dd} = \frac{h}{g\beta\pi T_{2dd}} \tag{1}$$

$$\frac{1}{T_{2dd}} = \frac{3}{20}\gamma^4\left(\frac{h}{2\pi}\right)^2\frac{1}{r^6}\tau\left(3 + \frac{5}{1+\nu^2\tau^2} + \frac{2}{1+4\tau^2\nu^2}\right) \tag{2}$$

where γ is the gyromagnetic ratio of the electron, τ is the correlation time of the interspin vector, ν is the frequency of the microwave radiation, and the other quantities are as defined above. Thus, this rotational dipolar relaxation mechanism predicts a homogeneous Lorentzian line broadening proportional to $1/r^6$, as observed experimentally for the T4L double mutants (Figure 9). Earlier studies verified the rotational dipolar relaxation mechanism for relaxation in nitroxide biradicals (Michon & Rassat, 1974) and for the similar process of metal ion−nitroxide relaxation, where T_{1e} relaxation of the metal ($T_{1e} \approx 3$ ns) provides the stochastic relaxation process rather than rotational motion of the interspin vector (Leigh, 1970; Voss et al., 1995). The rotational dipolar relaxation mechanism is necessarily operative in the doubly labeled T4L mutants and produces relatively large effects. For example, taking a τ_c of 6 ns, Eqs 1 and 2 predict a line broadening of ≈3 G for $r = 15$ Å, easily detectable on the ≈3 G line widths in the spin-labeled protein.

The EPR line shapes of all of the single mutants listed above correspond to nitroxides near the fast motional limit, as can be seen from the sums of the single mutants in Figures 4a and 8 (note that the spectra in Figure 6 were recorded in 30% sucrose and cannot be compared to those in Figures 3, 4, and 8). In this motional regime, spectral anisotropies have been averaged, and the homogeneous line widths are determined by modulation of anisotropic hyperfine and Zeeman interactions due to molecular rotation (McConnell, 1956).

For the doubly labeled proteins studied here, relaxation due to rotational modulation of both dipolar interactions and anisotropic Zeeman and hyperfine interactions must be considered. Although it may be necessary to consider these mechanisms together in a rigorous solution to the relaxation problem, we note here that the experimental data in Figure 9 can be accounted for by assuming that the relaxation mechanisms can be treated independently, that is,

$$\Delta H_o = \Delta H_{A,g} + \Delta H_{dd} + \Delta H_i \tag{3}$$

where ΔH_o is the overall line width and $\Delta H_{A,g}$, ΔH_{dd}, and ΔH_i are the contributions from modulation of hyperfine and Zeeman interactions, modulation of dipole−dipole interaction, and the intrinsic (inhomogeneous) line width of the nitroxide, respectively.

With this assumption, ΔH_{dd} is identified with ΔH of Figure 9, and the apparent interspin distance can be directly computed from eqs 1 and 2. The interspin distances determined in this manner with a τ_c of 6 ns (R_{calc}) are compared to the distances predicted from modeling (R_{model}) in Figure 10. The width of the horizontal bar reflects estimated uncertainty in the distances determined from modeling (see Materials and Methods). The agreement is good and suggests that, within experimental error, the rotational dipolar relaxation mechanism is sufficient to account for the spectral broadening.

DISCUSSION

General Strategy for Detection of Conformational Changes. Structural rearrangements in proteins may involve rigid body motions of secondary structural elements or entire domains, either of which necessitate repacking along tertiary contact surfaces (Gerstein et al., 1994). In this paper, we explore two means of detecting such changes in T4L: (1) changes in inter-residue distances and (2) changes in the mobility of nitroxide side chains located at or near tertiary contact surfaces.

Conformational changes can be directly studied through inter-residue distance changes, which can be estimated in SDSL through changes in magnetic interactions between nitroxide side chains in doubly spin-labeled proteins. Measurement of the distance between nitroxides in the rigid limit is well-established (Beth et al., 1984; Farahbakhsh et al., 1993; Rabenstein & Shin, 1995), and rigid limit conditions are readily achieved at low temperatures in frozen solutions. However, conformational equilibria may be strongly temperature-dependent, and the use of low temperatures is problematic. The results presented here show that nitroxide−nitroxide interaction in T4L is observed at room temperature as a simple spectral line broadening (ΔH) which may be used to qualitatively resolve different conformations in solution. With a sufficiently large number of spin pairs

designed to reveal patterns of distance changes, models for a conformational change can be critically evaluated.

In the context of the rotational dipolar relaxation mechanism, quantitative determination of the inter-nitroxide distance by the method used here is only possible for proteins with a sufficiently low molecular weight that the rotational motion effectively averages the static dipolar interaction and for nitroxides near the fast motional limit. The upper limit to molecular weight depends on the distance in question, but proteins in the range of 5000−30000 are amenable to study. However, a recently introduced method for distance determination between a metal ion in an engineered binding site and a nitroxide can be employed for larger proteins (Voss et al., 1995).

For the purpose of inter-residue distance determination, a pair of nitroxide side chains is introduced into the protein, preferably on solvent-exposed surfaces where structural perturbation is minimal (Matthews, 1993; Mchaourab et al., 1996). The relationship between the inter-nitroxide distance and the distance between the α-carbons of the spin-labeled residues depends on the conformation of the spin-labeled side chain. In favorable cases, where the structure of the protein is known, this relationship can be determined by modeling. Under any condition, a change in the inter-nitroxide distance for surface residues where the side chain conformation is invariant during a rigid body motion is expected to be a useful measure of backbone displacement. In the present work, multiple pairs of R1 side chains at surface sites are employed to evaluate *patterns* of distance changes relative to a reference state with a known structure, the T4L−substrate complex.

The mobility of nitroxide side chains is determined in part by constraints imposed by tertiary interactions. Thus, repacking along tertiary contact surfaces is expected to lead to changes in nitroxide mobility as reflected in the spectral line shape. Even though the structural perturbation due to the R1 side chain is minimal at most tertiary contact sites (Mchaourab et al., 1996), shifts in the relative populations of conformers with similar energy due to the nitroxide must be anticipated. Nevertheless, the solution conformation of T4L relative to the T4L−substrate complex revealed by changes in R1 mobility mirrors rather well those inferred from changes in inter-residue distances.

Conformation of T4L in Solution. The results presented here clearly demonstate a difference in conformation of T4L in solution with and without substrate bound. The nature of the difference is in accord with an opening of the active site cleft upon substrate removal due to hinge bending of the type observed in the various crystal structures of the protein. Thus, a population of T4L exists in solution that is more similar to the open structure observed in crystals of the I3P and M6I mutants than to the closed structure observed in crystals of T4L itself. Because patterns of distance changes at multiple pairs of sites and changes in tertiary interaction evaluated from single R1 side chains are all in agreement regarding the nature of the conformational change, it is unlikely that the changes observed are due to perturbations induced by the non-native R1 side chain.

As mentioned in the Results, some spectra for R1 pairs in the absence of substrate indicate a distribution of interspin distances, suggestive of a conformeric equilibrium. Because the multiple conformations of the protein observed in various crystal structures must have similar energies, an equilibrium mixture in solution is in fact expected.

In order to clearly discern spectral components arising from multiple distances, the spectral breadths, and hence interspin distances, of the individual components must be sufficiently different. This is the case for an equilibrium involving open and closed conformations for F4R1/K60R1, D22R1/R137R1, and F4R1/V71R1, where the spin pairs are in close proximity in one state and far apart in the other (Figures 2 and 4). In these cases, the spectra indeed reveal multiple populations. This is striking in the case of F4R1/K60R1, where two spectral populations are resolved, and in D22R1/R137R1, where the broad wings of the spectrum provide evidence of multiple populations. For F4R1/V71R1, the presence of two components is not obvious. This results from the great breadth of the spectrum in the closed state and a dominance of the narrow components characteristic of the open state. The presence of a broad underlying component is apparent upon amplification of the vertical scale (not shown). In the spectra of D22R1/T109R1, K35R1/T109R1, and K35R1/R137R1, multiple components are not obvious upon visual inspection of the spectra. This is consistent with the model of an equilibrium between open and closed states, because the differences in distances between the two states in D22R1/T109R1 and K35R1/T109R1 are not sufficiently great to permit obvious spectral resolution, and the unusually sharp lines of K35R1/R137R1 in the open state probably dominate the considerably broader lines of the closed state. It is for this reason that K35R1/R137R1 was selected for inter-nitroxide distance determination in the open state.

Although the above arguments were constructed with reference to a two-state equilibrium, there is likely to be a continuous distribution of conformations corresponding to a range of hinge bend angles because the energy differences between the states involved are small. In the absence of specific data on the spectral line shapes as a function of the hinge-bending angle, it is not profitable to attempt to quantitatively analyze the spectra in terms of equilibrium distributions. In addition, even weak perturbations due to the presence of the R1 side chain could significantly affect the distribution of states that differ little in energy. However, the results do clearly argue in favor of the existence of conformeric equilibria, with an open conformation being predominant.

Mechanisms of Spin−Spin Interaction and Distance Measurements. The rotational dipolar relaxation mechanism is necessarily operative in the T4L double mutants, and the good correspondence between R_{calc} and R_{model} shown in Figure 10 indicates that it alone is sufficient to account for the data. However, this does not prove that it is the only operative mechanism of line broadening. The correlation time of T4L is on the limit of applicability of eq 2, close to the regime where static dipolar interactions contribute. With regard to this point, we note that the interspin distance in the double mutant K65R1/Q69R1 is predicted to be ≈9 Å. At this close distance, both static and dynamic dipolar contributions to the line width are expected, as well as a contribution from exchange. Nevertheless, the spectrum is fit well by eqs 1−3, with a distance in agreement with that determined from molecular modeling. This spectrum is quite unlike that obtained by Fiori et al. (1993) for the R1 side chains at adjacent turns of a helix in a small peptide, because the short correlation time of the peptide effectively averages static dipolar contributions, and the dynamic dipolar relaxation contribution is much smaller (it is linear in τ_c).

Static dipolar interactions at K65R1/Q69R1 will also lead to line broadening. Because distances are related to the inverse sixth root of the line broadening, the calulated distances are not very sensitive to additional contributions to ΔH arising from unaveraged static dipole contributions. This may at least partly account for the unexpected agreement of R_{calc} with R_{model} at K65R1/Q69R1.

Some of the mutants have interspin distances in the neighborhood of 12−13 Å, where exchange interactions may lead to line broadening of up to ≈3 G (Fiori & Millhauser, 1993), although more recent estimates suggest that it may be much less (Fiori & Millhauser, 1995). Under any circumstance, line broadening from the rotational dipolar relaxation mechanism in T4L at this distance is ≈12 G, clearly dominating. Again, the effect of even an additional 3 G of broadening is lost in taking the sixth root to compute the distance, and the presence of weak exchange interactions will not be detected as deviations from the model presented. Beyond about 14 Å, exchange is completely negligible compared to the rotational dipolar relaxation contribution.

The dipolar interaction may be modulated through time-dependent changes in r as well as by molecular tumbling. The former contribution has not been considered here because the latter alone can account for the data. In addition, previous work has indicated that the motion of the nitroxide in R1 is relatively restricted due to interactions of the disulfide with the protein (Mchaourab et al., 1996), reducing the importance of distance modulation. A similar conclusion was reached by Fiori and Millhauser (1995).

The data presented above show that, for a protein correlation time of ≈6 ns, the range of spin−spin interaction is from van der Waal's contact to about 25 Å. It is interesting that this is roughly the same range as static dipolar interactions between nitroxides in frozen solutions (Rabenstein & Shin, 1995), although the distance in that case is dependent on $1/r^3$ and one would expect the interaction to be longer range. It is indeed longer range, but the broad lines in frozen solutions limit the sensitivity for detection of small degrees of broadening with respect to the sharp lines observed in solution at room temperature.

The primary use of the method presented here will be to identify probable ranges of interspin distances and their changes. Clearly, for T4L, one can deduce without calculation that extensively broadened lines such as those observed for K65R1/Q69R1, D22R1/R137R1, and F4R1/V71R1 originate from spins at an $r \leq 10$ Å separation. A weak interaction implies an r of ≥ 20 Å, and intermediate degrees of broadening necessarily fall in the range of 12−17 Å. For many purposes, this is already sufficient information. It must be emphasized that, if the rotational dipolar relaxation mechanism is correct, these limits will depend on the protein correlation time and must be scaled appropriately.

Finally, we point out that the ability to detect distance-dependent spin−spin interactions at room temperature opens the possibility of time-resolving distance changes during conformational transitions or protein folding. The first application of the latter has recently appeared (Hubbell et al., 1996).

ACKNOWLEDGMENT

The authors thank Dr. Yanliang Zhang for help on mutagenesis, Dr. John C. Voss for helpful suggestions, and Drs. Dave Farrens and Christian Altenbach for helpful discussions and critical reading of the manuscript.

REFERENCES

Abragam, A. (1961) *Principles of Nuclear Magnetism*, Oxford University Press, Oxford.
Arnold, G. E., Manchester, J. I., Townsend, B. D., & Ornstein, R. L. (1994) *J. Biomol. Struct. Dyn. 12*, 457−474.
Bennett, W. S., & Huber, R. (1984) *CRC Crit. Rev. Biochem. 15*, 291−386.
Bennett, W. S., Jr., & Steitz, T. A. (1978) *Proc. Natl. Acad. Sci. U.S.A. 75*, 4848−4852.
Beth, A. H., Robinson, B. H., Cobb, C. E., Dalton, L. R., Trommer, W. E., Birkoft, J. J., & Park, J. H. (1984) *J. Biol. Chem. 259*, 9717−9728.
Dixon, M. M., Nicholson, H., Shewchuk, L., Baase, W. A., & Matthews, B. W. (1992) *J. Mol. Biol. 227*, 917−933.
Faber, H. R., & Matthews, B. W. (1990) *Nature 348*, 263−266.
Farahbakhsh, Z., Hideg, K., & Hubbell, W. L. (1993) *Science 262*, 960−963.
Farahbakhsh, Z., Huang, Q.-L., Ding, L.-L., Altenbach, C., Steinhoff, H.-J., Horwitz, J., & Hubbell, W. L. (1995) *Biochemistry 34*, 509−516.
Farrens, D. L., Altenbach, C., Yang, K., Hubbell, W. L., & Khorana, H. G. (1996) *Science 274*, 768−770.
Fiori, W. R., & Millhauser, G. L. (1995) *Biopolymers 37*, 421−431.
Fiori, W. R., Miick, S. M., & Millhauser, G. L. (1993) *Biochemistry 32*, 11957−11962.
Gerstein, M., Lesk, A. M., & Chothia, C. (1994) *Biochemistry 33*, 6739−6749.
Hubbell, W. L., & Altenbach, C. (1994) *Curr. Opin. Struct. Biol. 4*, 566−573.
Hubbell, W. L., Mchaourab, H. S., Altenbach, C., & Lietzow, M. A. (1996) *Structure 4*, 779−783.
Kuroki, R., Weaver, L. H., & Matthews, B. W. (1993) *Science 262*, 2030−2033.
Leigh, J. S. (1970) *J. Chem. Phys. 52*, 2608−2612.
Matthews, B. W. (1993) *Annu. Rev. Biochem. 62*, 139−160.
McConnell, H. M. (1956) *J. Chem. Phys. 24*, 764−767.
Mchaourab, H. S., Lietzow, M. A., Hideg, K., & Hubbell, W. L. (1996) *Biochemistry 35*, 7692−7704.
Michon, J., & Rassat, A. (1974) *J. Am. Chem. Soc. 96*, 335−337.
Petsko, G. A., & Ringe, D. (1984) *Annu. Rev. Biophys. Bioeng. 13*, 331−371.
Rabenstein, M. R., & Shin, Y. K. (1995) *Proc. Natl. Acad. Sci. U.S.A. 92*, 8239−8243.
Smirnov, A. L., & Belford, R. L. (1995) *J. Magn. Reson. A113*, 65−73.
Steinhoff, H., Mollaaghababa, R., Altenbach, C., Hideg, K., Krebs, M., Khorana, H. G., & Hubbell, W. L. (1994) *Science 266*, 105−107.
Timofeev, V. P., & Tsetlin, V. I. (1983) *Biophys. Struct. Mech. 10*, 93−108.
Voss, J., Salwinski, L., Kaback, R., & Hubbell, W. L. (1995) *Proc. Natl. Acad. Sci. U.S.A. 92*, 12295−12299.
Wagner, G., Hyberts, S. G., & Havel, T. F. (1992) *Annu. Rev. Biophys. Biomol. Struct. 21*, 167−198.
Weaver, L. H., & Matthews, B. W. (1987) *J. Mol. Biol. 193*, 189−199.
Zhang, X., Wozniak, J. A., & Matthews, B. W. (1995) *J. Mol. Biol. 250*, 527−552.

BI962114M